Slovak University of Technology in Bratislava,
Faculty of Civil Engineering

Ing. Andrej Hideghéty

Dissertation Thesis Abstract

Online deformation measurement using 2D photogrammetry

to obtain the Academic Title of Philosophiae doctor (PhD.)

in the doctorate degree study program:

3636 Geodesy and Cartography

in the field of study:

3636 Geodesy and Cartography

Form of Study:

full-time

Bratislava 2023

Dissertation Thesis has been prepared at

Slovak University of Technology in Bratislava, Faculty of Civil Engineering,

Department of Surveying

Submitter:	Ing. Andrej Hideghéty Department of Surveying Faculty of Civil Engineering, STU in Bratislava Radlisnkého 11, 810 05 Bratislava
Supervisor:	doc. Ing. Marek Fraštia, PhD. Department of Surveying Faculty of Civil Engineering, STU in Bratislava Radlisnkého 11, 810 05 Bratislava
Readers:	prof. Dr. Ing. Karel Pavelka Department of Geomatics Faculty of Civil Engineering, CTU in Prague Thákurova 7, 166 29 Praha 6
	doc. Ing. Juraj Gašinec, PhD. Institute of Geodesy, Cartography and GIS Faculty of Mining, Ecology, Process Control and Geotechnologies, TU in Košice Park Komenského 19, 040 01 Košice
	doc. Ing. Bc. Miroslav Kardoš, PhD. Department of Forest Resource Planning and Informatics Faculty of Forestry, TU in Zvloen Masaryka 24, 96001 Zvolen

Dissertation Thesis Abstract was sent: 30.06.2023

Dissertation Thesis Defence will be held on 24.08.2023

at 8:00h am at the Department of Surveying, Faculty of Civil Engineering, STU in Bratislava, Radlinského 11, 810 05 Bratislava.

prof. Ing. Stanislav Unčík, PhD.

Dean of the Faculty of Civil Engineering, STU in Bratislava

Introduction

Photogrammetric methods are increasingly being utilized for the measurement of displacements and deformations. High-end digital cameras, as well as computer components, are becoming more widely accessible as science and technology progress. Most professional cameras already have built-in Wi-Fi systems for data transmission. The field of data transmission via wired connections has also undergone significant advancements. Multi-core processors with high frequencies and huge operational memories are available not only in desktop computers but also in laptops, facilitating faster data processing in the field. Displacement and deformation measurements are essential when assessing the safety and operability of bridges and structures in general. It is essential to maintain deformations within acceptable limits to guarantee the bridge's functionality. Load tests are required to check the reliability of the bridge structure to prevent collapse or major deterioration of its condition. The utilization of a unique method, referred to as time base photogrammetry, is investigated in this study. A set of certain conditions that need to be satisfied for this method to function optimally is outlined in the initial segment of the study. Alongside these conditions, practical implementations used to fulfill them, as well as the tests conducted to ascertain their effectiveness, are also detailed. The subsequent section of the thesis describes how the findings and practical implementations derived from the initial part of the study are integrated into an algorithm developed by the author. This algorithm, equipped with online capabilities, is used for the accurate measurement of object deformations. Here, 'online' refers to the real-time data processing conducted with minimal delay and simultaneous to the ongoing image acquisition process. This section provides detailed accounts of the online measurements taken, as well as an explanation of the operational functionality of the MATLAB code, which was specifically developed for this research. The objective of this section is to offer a comprehensive understanding of the applicability of time base photogrammetry in online deformation measurements.

Literature Review

Non-contact imaging techniques, as compared to contact methods, potentially offer greater benefits in the measurement of displacements and deformations. They enable measurements to be conducted from a specific distance and provide the possibility for complete automation in data processing, along with online analysis of results [1]. Nevertheless, the adoption of these techniques has been rather recent. Abolhasannejad et al. [2] defined the movement of the investigated object as local motion and the movement of the camera due to external influences as global motion. Their algorithm started by defining a square Region of Interest (hereafter ROI), within which the occurrence of local movement on the image was not assumed, that is, a part of the fixed background was selected on the image. This ROI had to contain fixed points, based on which they corrected the global movement of the camera in the ROI and thereby stabilized it analytically [2]. Using ROI-based analytical stabilization is the main benefit of this study. In a laboratory experiment, Fraštia utilized time-lapse photography with a Nikon D800E camera to capture 10 images over the course of 10 minutes without any manipulation. Camera shakes were observed only due to shutter release. The resulting circle diameters varied between 10-8 pixels. The Photomodeler Scanner software was used for Least-Squares Matching (LSM) analysis and showed that the total mean error when searching for target mark centers was σ_X=σ_Y=0.03 pixels [3]. For the field test conducted on a bridge object, eight pictures were taken at intervals of 20 minutes using the stakeout network's pillar as support. Fixed points on the background were semi-automatically measured by a circular operator, which had an average repeatability error of ±0.23 pixel along with maximum differences ranging from -0.20 pixel to +0.34px indicating positional and height changes [3]. The next stage involved measuring points of interest which are utilized for the automatic alignment of images. These points are created through a specific image detector, and it is assumed that identical points will be generated for an unchanging image. However, the exact detector used by Photomodeler Scanner (PMS) remains unknown. The positioning error on these identified points had an average of 1.77 pixels, with maximum deviations ranging from -2.62 to +2.55 pixels, indicating low accuracy in the generated interest point detector within the PMS system. Test results highlighted that high levels of precision can be achieved using circular operators in laboratory conditions (0.05 pix) and field conditions (0.3 pix). Considering this discovery, it was revealed that due to their inaccurate nature (ranging between 1-3 pixels), identifying interest points via PMS is impractical A technical review about vision-based deflection measurement of bridges published by Jinke Huang et al. [4] lists the most relevant deformation measuring methods and emphasizes the importance of visual-based methods. In this study, a range of photogrammetric methods were mentioned: two-dimensional measurement with a single camera, three-dimensional measurement with dual cameras, quasistatic deflection measurement based on monocular photogrammetry, multipoint dynamic measurement based on displacement-relay videometrics, and deflection measurement based on a UAV platform. For the purposes of this thesis, measurements using a single camera and monocular photogrammetry are the most relevant. The study also summarizes the factors that influence the measurements. These are the following:

1. Camera factors
2. Calibration factors
3. Algorithm factors
4. Environmental factors

Objectives of the Dissertation

Given the current status of the matter and the comprehensive literature review, it is clear that the methodology of time base photogrammetry presents considerable potential for exploration, particularly when the goal involves achieving superior accuracy in deformation and displacement measurements utilizing this approach. Consequently, the objectives of this dissertation thesis were articulated during the dissertation examination as follows:

Main goal: Design and implementation of a system for online processing of photogrammetric measurements of displacements and deformations.

Specific objectives:

1. Design of the optimal method of data transfer from the camera to the computer.
2. Selection of a suitable image operator and edge detector and their implementation, including subpixel measurement of target centers.
3. Hardware and analytical camera stability solution.
4. Graphical user interface design for data collection and processing.
5. Experimental verification of the system.
6. Analysis of the quality of measured data and the accuracy of displacements and deformations.

1 Measurement of Deformations and Displacements of Building Structures and Bridges

In the construction of any building, internal and external forces can impact its geometric parameters and technical equipment. This often leads to sinking foundations and changes in the supporting structures of the building. The uneven settling of foundations is a common issue that may cause significant disturbances in stability, potentially resulting in static failures or even the total collapse of the building. To ensure safe construction practices and operational functionality, it is necessary to regularly measure shape and size parameters for both foundation structures and supporting elements.

1.1 Required Accuracy of Measurements

The accuracy of displacement measurements depends mainly on the size and nature of the displacements. Sufficient accuracy in displacement measurement can be considered the accuracy that guarantees the achievement of the goal with minimal measurement costs [6]. In this case, the accuracy of measurement will be defined according to the Slovak Technical Norm STN 73-0405. Measurement of deformation of building constructions:
The accuracy of measuring displacements of building objects is characterized by the value of the basic standard deviation σ p to determine the amount of displacement, i.e., the length of the vector, which is a geometric representation of displacement. The accuracy of displacement measurement can also be expressed by the standard deviation for determining the displacement component in the direction of the coordinate axes (σ_{px}, σ_{py}, σ_{pz} or σ_{pH}) or in the direction characteristic of the measurement object or its parts (transverse or longitudinal shift, shift in the direction of one of the axes or a characteristic line object, or in the direction perpendicular to these axes or lines). The value of the basic standard deviation σ p is determined, unless specified otherwise, according to the formula:

$$\sigma_P = \frac{1}{15} . |p|, \tag{1-1}$$

Where $|p|$ is the absolute value of the total expected displacement or its component.
The value of the basic standard deviation of measurement of vertical displacements in new buildings (during their construction or up to 1 year after their approval) shall not exceed the following values:

a) $\sigma_h = 0{,}5\ mm$ for buildings where the foundation soil is predominantly composed of rocky and semi-rocky formations,
b) $\sigma_h = 1{,}0\ mm$ for buildings where the foundation soil is predominantly composed of sandy, clayey, and other compressible soils and compacted fills,
c) $\sigma_h = 2{,}5\ mm$ for buildings where the foundation soil is predominantly composed of uncompacted fills and highly compressible soils.

The value of the basic standard deviation of measurement of displacements of buildings in use or in operation that are affected by construction activities in their vicinity shall not exceed the value:

$$\sigma_p = \frac{1}{5} \cdot |p_k|, \quad (1\text{-}2)$$

where $|p_k|$ is critical displacement value in millimeters, defined as the point at which the construction object becomes endangered.

1.2 Geodetic Methods

Geodetic methods for measuring displacements are often used in practice [5]. The methods for measuring vertical displacements are as follows: The method of geometric leveling is most often used to measure vertical displacements. The principle is based on periodically repeating the leveling of the observed points located on the measured object. It follows from theoretical and practical experience that the empirical mean measurement error of vertical displacements σ_n= 0.15 mm to σn= 0.30 mm can be achieved by the very precise leveling method. The following geodetic methods are used to measure horizontal displacements [5]: The measuring-line method is used to measure horizontal displacements of observed points. The method is quite simple and fast. In practice, the most commonly used method is the one using a sliding target with a linear scale or the method by measuring the parallax angles between reference and observed points. The accuracy of determining displacements is 0.2 mm to 0.4 mm. The accuracy of this method combined with the optoelectronic reading of the laser track ranges from 0.1 mm to 0.5 mm [5].

Compared to the measuring line, the trigonometric method is more laborious, more expensive, and more demanding on the professional level and skill of the workers. However, it has advantages over the intentional measuring line in that it provides information about the displacement in two, respectively in several ways. Allows you to determine the displacement of the object, or its parts even in inaccessible places. Based on many years of experience with the application of this method, the accuracy of determining the displacements can be expected between 0.5 mm to 1.0 mm. The decisive factor in the application of the trigonometric method is the shape and method of stabilizing the network of reference points, or the accuracy of determining its parameters. No less important is the distance of reference points from the object of measurement [5]. Measuring systems equipped with software and special accessories are used to measure displacements with high precision (0.05 mm to 0.30 mm), which is required especially in the field of mechanical engineering, e.g., targets, self-adhesive films, etc. To achieve complete automation of the measurement process and accuracy below the 0.1 mm limit, interferometers are used in special cases to measure lengths. This creates dynamic measurement systems capable of tracking a target moving in space at a speed of up to $5\ \mathrm{m} \cdot \mathrm{s}^{-1}$. The measurement of horizontal displacements by the polar method is possible if we have available universal stations with the accuracy characteristics σ_S= 1+1 ppm and $\sigma_\alpha = 3^{cc}$, and the target lengths do not exceed the value of 100 m. When using a device with a servo drive, the measurement can be fully automated. The polar method is used mainly for measuring displacements of smaller objects, or constructions [5].

1.3 Methods of Close-range Photogrammetry

Close-range photogrammetry is a widely applicable measurement technology due to its ability to capture both the geometry and radiometric properties of objects through optical imaging. This type of recording closely resembles human vision, making it an attractive option for various purposes requiring 2D or 3D reconstruction. The automation of digital image processing presents significant potential and possibilities in this field, with ongoing global developments in algorithms driving progress forward without any apparent limits. [3].

Photogrammetric approaches can be categorized by the camera's location with respect to the subject, the distance between them, the processing methodology, and other factors. The methods are the following: Projective photogrammetry, time base photogrammetry, convergent photogrammetry and photoscanning – Structure from motion

2 Time Base Photogrammetry

This chapter will focus on the measurement of displacements using time base digital photogrammetry in the context of online deformation measurements. Theoretical prerequisites are mainly drawn from the habilitation thesis of doc. Ing. Marek Fraštia, PhD. [3].

The fundamental benefit of this method is its simplicity, especially when using low-cost photographic and software equipment, and the possibility to simultaneously record a high number of points in a single image, which is unachievable using traditional geodetic methods. This method can be primarily used during load tests of bridges and other objects, and basically in any application where deformations and displacements must be measured either with a temporal delay or in real time [3]. To sum up, achieving subpixel accuracy requires the following theoretical and practical assumptions to be adhered to:

1. Utilization of a target measuring operator boasting an accuracy exceeding 0.1 pixel.
2. A high degree of spatial and geometric resolution.
3. Superior image quality.
4. Ensuring that the image plane aligns parallel to the deformation plane.
5. Constant EOP and IOP, implying a stable camera.
6. Accurate computation of the scaling factor.
7. Images that have been corrected for lens distortion.

These outlined conditions serve not only as prerequisites but also form an integral part of the objectives of this dissertation. Each condition, being a prerequisite for precise measurements, along with their practical realization will be elaborately expounded in the subsequent subsections.

2.1 Image operators

The accuracy of image coordinate measurements directly affects the accuracy of the displacement in the reference space. If the image operator has an accuracy of 0.05 pixels in ideal conditions, it is expected that the resulting accuracy will be lower in real-world outdoor use because of other factors [3]. For this reason, it is important to establish the method applied in this thesis and its accuracy. Luhmann et al. [7] list a range of point-measuring methods, such as *centroid methods*, *correlation methods*, *Least-squares matching* and *ellipse operators*.

Digital Image Correlation engine (DICe) is an open source DIC tool intended for use as a module in an external application or as a standalone analysis code. Its primary capabilities are computing full-field displacements and strains from sequences of digital images and rigid body motion tracking of objects. The images analyzed are typically of a material sample undergoing a characterization experiment, but DICe is also useful for other applications, such as trajectory tracking [8]. The accuracy of this method is later tested in this thesis on real images.

Least-squares matching employs an iterative geometric and radiometric transformation between the reference image and the search image to minimize the least-squares sum of grayvalue differences between both images. The reference image can be a window in a real image that must be matched in a corresponding image. For a known gray value structure, the reference image can be generated synthetically and used as a template for all similar points in the search image. The geometric fit assumes that both image patches correspond to a plane area of the object. The mapping between two central perspective images can then be described by the 8-parameter projective transformation, or 6-parameter affine transformation for small image patches. The radiometric fit is performed by a linear gray value transformation with two parameters.

After performing comparative investigations of different measuring algorithms applied to synthetic and real test images, the following conclusions were drawn [7]: For real imagery with well exposed and bright elliptical targets, accuracies of 0.02 – 0.05 pixel can be achieved if least-squares operators or adaptive centroid operators are applied to multi-image configurations. Ellipse measurement based on edge detection tends to be slightly more accurate than least-squares matching and centroid methods if there is increased image noise or distinct blunders present. A pivotal factor in determining the accuracy of points is the size of the points being captured. The ideal target size typically falls within a diameter range of approximately 5 to 15 pixels. Points smaller than this may not provide sufficient object information, which can limit the precision of matching procedures or edge-based operators. On the other hand, while larger point diameters result in a greater number of observations, the number of significant edge points only increases linearly. In contrast, the number of pixels in the window increases quadratically. Furthermore, as the size of the points increases, disturbances in the image become more likely, which could potentially displace the center of the ellipse relative to the actual center of the target circle [7]. To achieve subpixel accuracy while locating the center of the ellipse it is evident that the edge detection algorithm should also perform with subpixel accuracy.

2.1.1 Edge-ellipse operator for online deformation measurements

The operator used for the online deformation measurement algorithm is based on ***accurate subpixel edge location based on partial area effect*** developed by Agustín Trujillo-Pino et al. [28, 29] and *fitellipse*, a least-squares ellipse fitting function developed by Richard Brown [11]. Most works in the literature assume that a digitized image F is the sampled version of a function $f(x, y)$ over a rectangular grid of pixels. To apply differential calculus techniques on the image, it is also assumed that f is continuous and differentiable inside its domain. This edge detection method was used because it detects edges with subpixel accuracy and assumes that an edge is a curve, not a straight line.
The **Edge-ellipse operator by Hideghéty** consists of an in-house approach based on the subpixel edge detection method described earlier in combination with *fitellipse*. Let us consider a single circular target in the image taken during a load test of a bridge. The simplified workflow is performed as follows:

1. The image is undistorted according to the calibration protocol.
2. A rectangle is drawn around the target, and an ID is assigned to the target.
3. The entire image is converted to grayscale.
4. The value of the top left corner pixel of the rectangle is assigned to all pixels outside the boundary of the rectangle, and the result is stored as `valueImage`.
5. Threshold metering is performed, or a fixed threshold value is assigned.
6. Edges are detected with subpixel accuracy according to the threshold.
7. Using *fitellipse* an ellipse is fitted over the edge points.
8. ID and center coordinates of the ellipse stored.

2.1.2 Testing the Edge-ellipse operator

The effectiveness of an image operator is largely dictated by the image quality, which is inherently determined by the camera used for data acquisition and its associated settings. Therefore, a discussion regarding the performance and precision of an image operator should be contextualized within the specific camera used. Trials were conducted using four unique camera configurations; however, this section will primarily focus on the results obtained with the Nikon D850 with a 35 mm lens. The first experiment was conducted with the camera securely mounted on a steel plate, stationed 1.7 meters away from a target board. This board showcased targets of four distinct sizes. With a GSD of 0.21 mm, the 10-, 5-, 2-, and 1-millimeter targets correspondingly span 50, 25, 10, and 5 pixels in diameter. Using silent shooting mode, an image was captured every minute over a span of 240 minutes. This mode, by eliminating the shutter's clapping sound, theoretically minimizes the incidence of potential error caused by vibration. The experiment was carried out within a controlled laboratory environment. The specific configuration adopted for this experiment is illustrated in figure 2.1.

Fig. 2.1 Configuration of the experiment (left), camera's point of view (middle) and a close-up of the target board (right)

The key aspect of this configuration is the guaranteed stability of both the camera and the target board, made possible by ensuring neither is tampered with and that the connecting plate remains rigid. This setup maximizes the camera's steadiness. Theoretically, alterations in X and Y image coordinates should be nonexistent, yet in practice, empirical changes may slightly deviate from zero. The X-axis represents the horizontal coordinates, and the Y-axis represents the vertical coordinates in a landscape-oriented image coordinate system. The origin is at the top left corner of the image. The measured changes in the X and Y coordinates of two 50-pixel targets are shown in fig. 2.2.

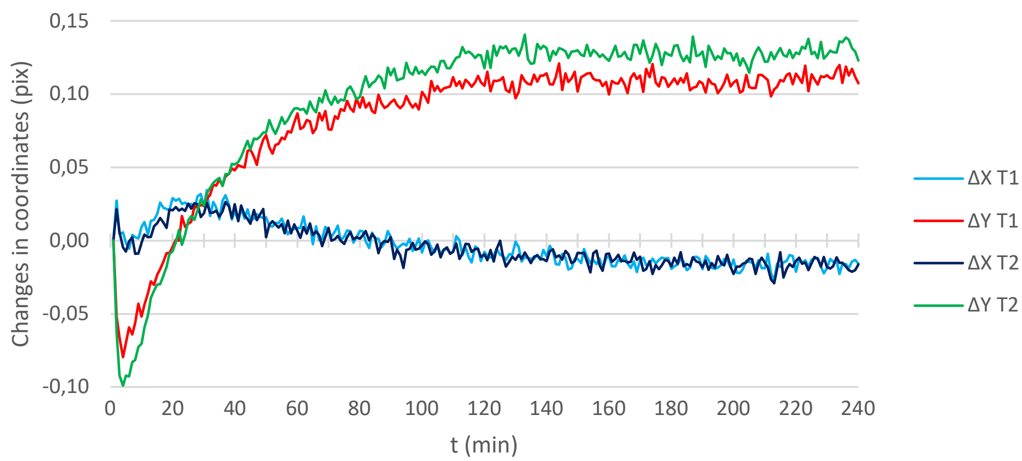

Fig. 2.2 Changes in image coordinates for targets T1 and T2, with a dimeter of 50 pixels

Two notable observations were made following the initial experiment. First, changes in the X image coordinates exhibit a sharp peak and dip within the initial few minutes, followed by a gradual rise over the first 20 minutes, a prolonged decline, and finally stabilizing after approximately 120 minutes. The Y coordinate changes, on the other hand, dip sharply before rising steadily for 120 minutes and subsequently leveling off.

The second observation involved discrepancies in the behavior of the Y coordinates between the two targets, despite them being affixed to the same panel. This divergence has also been noted by several authors [33, 34, 35] and attributed to the self-heating effect of the sensor. To investigate this phenomenon further, an additional experiment was conducted. A Nikon D850 camera was mounted on a tripod, with the lens detached to expose the sensor directly. The camera was programmed to capture an image every minute for a duration of 220 minutes. Simultaneously, a FLIR T620 [15] infrared camera, positioned facing the D850, captured thermal images of the D850 sensor at the same interval. In time base photogrammetry, the changes in Y coordinates represent the vertical deformations, therefore, these coordinates were correlated with the temperature of the sensor. The Pearson correlation coefficient [16] between the changes in Y coordinates and the measured temperature of the sensor is 0.95, indicating a very strong positive linear relationship between these two datasets.

2.1.3 Accuracy of the Edge-ellipse operator, impact of target size

The experiments continued with capturing a pair of targets of each diameter as previously explained; however, due to the self-heating phenomenon observed in the first 120 minutes of the experiment, these measurements were cut for now from the evaluation, as this section examines the raw potential of the Edge-ellipse operator under ideal conditions. The statistical analysis for each target pair is shown in table 2.1.

Tab. 2.1 Statistics of changes in image coordinates for different marker sizes

Statistics for t=120 min until t=240 min (pix)										
Size	Mean value		Standard deviation		Root mean Square		Min		Max	
	X	Y	X	Y	X	Y	X	Y	X	Y
50	-0.004	-0.006	0.004	0.005	0.006	0.008	-0.016	-0.018	0.010	0.006
	-0.001	-0.001	0.005	0.005	0.005	0.005	-0.016	-0.015	0.013	0.011
25	-0.007	-0.004	0.006	0.006	0.009	0.007	-0.020	-0.022	0.017	0.014
	-0.004	0.000	0.005	0.005	0.007	0.005	-0.017	-0.010	0.009	0.016
10	-0.012	0.001	0.008	0.007	0.015	0.007	-0.033	-0.016	0.011	0.018
	-0.009	-0.001	0.008	0.008	0.012	0.008	-0.032	-0.026	0.009	0.017
5	-0.008	0.019	0.008	0.012	0.011	0.022	-0.028	-0.002	0.013	0.051
	-0.017	0.021	0.009	0.009	0.019	0.023	-0.034	0.000	0.006	0.051

The potential accuracy of the Edge-ellipse operator for measuring vertical deformations is under 0.01 pixel with the D850 camera and the AF-S DX NIKKOR 35mm f/1.8G.

2.1.4 Edge-ellipse vs LSM vs DICe

Similarly, as in section 2.1.2.1, the image coordinates of a target of each dimension were measured first in MATLAB using the Edge-ellipse operator, then in Photomodeler [17] using the LSM operator, and finally with DICe, the open-source software for DIC. Again, the first 120 measurements were cut from the statistical analysis of this experiment because of the sensor's self-heating effect.

In comparing the three operators, the Edge-ellipse algorithm demonstrated the lowest RMS value at 0.0065 pixels for the 50-pixel diameter target. It performed slightly worse with a 25-pixel diameter target, registering an RMS value of 0.0068 pixels. As the target diameter decreased, both the RMS and the sum of the absolute minimum and maximum values increased. Yet, even for the smallest 5-pixel diameter target, the RMS value remained as low as 0.0166 pixels.

The DIC operator showed slightly superior performance when measuring the 25-, 10-, and 5-pixel diameter targets. While the LSM operator outperformed others for the 25-pixel diameter targets, it was incapable of measuring the 5-pixel diameter targets. Variations around zero appear to be random.

A comparison of the operators was additionally carried out using images from a load test conducted on a concrete beam. Such a test involves applying a load to the beam and assessing its corresponding response, with the goal of determining the beam's load-carrying capacity and behavior under varying loading conditions

The null hypothesis that the inliers follow a normal distribution was tested using the Jarque-Bera test, and the results indicate that the test rejects the null hypothesis at the 5% significance level with *p* values under 0.001.

In conclusion, when compared to LSM, the author's Edge-ellipse image operator produced competitive results; in 99.2% of the measurements, there was less than a 0.1-pixel difference between the two algorithms; therefore, the Edge-ellipse operator can be used in the author's online time base algorithm with great potential. The reliability of the detected edges was high, and the regression ellipse produced accurate results. 90% of DIC measurements differ by less than 0.15 pixels when compared to Edge-ellipse and LSM measurements; however, the presence of outliers indicates a potential correlation error that requires additional testing. It is possible that the correlation algorithm identified RAD targets similar to the one selected in the zero-state image.

2.1.5 Sensor sensitivity – ISO and shutter speed

ISO represents the sensitivity of the sensor, but high values can cause noise. To minimize noise, it is advisable to set the ISO to 400 [3]. In an experiment, 18 images were captured using aperture priority, meaning the aperture of the camera was constant and the ISO values were set by the user. In this mode, the shutter speed is calculated internally in the camera's software. The light conditions varied during the experiment to determine whether shutter speed impacts the accuracy of measurements. Based on the statistical analysis and the graphical interpretation of the vertical changes, there is no systematic correlation between the different shutter speeds or ISO values of up to 1000 and the changes induced in the coordinates. The subpixel edge detection function involves smoothing if needed for noisy images [11], and all tests and measurements performed in this thesis were performed using the default smoothing iteration applied to the images. This was performed because some circular targets appeared "dented" with no smoothing applied to the image - the detected edges appeared out of position. The default 1x smoothing produced desirable results, and 2x smoothing did not detect edges at the 3, 6, 9, and 12 o'clock positions of the circular target.

2.2 Spatial and geometric resolution

The theoretical accuracy of 0.05 pixels will be 0.35 mm for 25-pixel target, which in this case would be a circular target with a 185 mm diameter (25 x 7.4 mm).

Accuracy [mm]		D [m]									
		10	20	30	40	50	60	70	80	90	100
f [mm]	14	0.15	0.30	0.45	0.60	0.80	0.95	1.10	1.25	1.40	1.55
	20	0.10	0.20	0.35	0.45	0.55	0.65	0.75	0.85	1.00	1.10
	24	0.10	0.20	0.25	0.35	0.45	0.55	0.65	0.70	0.80	0.90
	28	0.10	0.15	0.25	0.30	0.40	0.45	0.55	0.60	0.70	0.80
	35	0.05	0.10	0.20	0.25	0.30	0.35	0.45	0.50	0.55	0.60
	50	0.05	0.10	0.15	0.15	0.20	0.25	0.30	0.35	0.40	0.45
	70	0.05	0.05	0.10	0.10	0.15	0.20	0.20	0.25	0.30	0.30
	80	0.05	0.05	0.10	0.10	0.15	0.15	0.20	0.20	0.25	0.25
	100	0.00	0.05	0.05	0.10	0.10	0.15	0.15	0.15	0.20	0.20

2.3 Image quality

During the measurement of image coordinates, edges are determined based on the differences in intensity at both sides of a given pixel, therefore, it is crucial to use an image file format that retains true intensity changes. RAW and TIFF formats are considered lossless formats that retain the full bit depth of the image, however, some applications might prefer JPEG because of the reduced file size despite the reduced image quality. The statistical analysis of differences shows that the differences between the file formats are minimal and consistent with the accuracy of the Sony A7RIII camera from the previous results. Also, it is best not to switch between file formats during measurements.

2.4 Orientation of image plane

Projective distortion does not occur when the displacement direction is parallel to the image plane. When äThe results indicate that the extreme tilting of the camera may cause changes in distances between points, and therefore changes in deformations, up to 1,5%, however a 1,5% change of small distances could be negligible at small deformations. A one-pixel displacement with extremely inaccurate tilt could still result in an accuracy of determining deformations better than 0,015 pixels. In conclusion, not having a perfectly horizontal optical axis impacts the measured deformations, however, the extreme tilt will likely never be present, as besides the virtual horizon, other methods can be used to level the camera, such as staking out the optical axis or using and external spirit level.

2.5 Camera stability

As demonstrated in section 2.1, measurements performed using the Edge-ellipse operator can achieve an accuracy of under 0.01 pixels, or at worst, 0.05 pixels when operating within the bounds of the statistical minimum and maximum. Given that the physical size of a pixel on a camera sensor is approximately 0.004 mm, the level of accuracy implies that the camera would have to remain stationary during the entire measurement campaign – moving less than 0.00004 – 0.00020 mm. Such precision is typically achievable only under specific laboratory conditions. Conversely, in scenarios where significant camera shake occurs, analytical stabilization might not sufficiently correct the acquired coordinates to guarantee their precision. Therefore, for optimal results, both physical and analytical stabilization of the camera should be pursued.

2.5.1 Physical stabilization

It's reasonable to expect that techniques adequate for stabilizing surveying equipment should also be sufficient for physically stabilizing a camera. This includes the use of heavy tripods and pillars. When applied appropriately, proper physical stabilization can effectively eliminate most significant movements and vibrations.

2.5.2 Analytical stabilization

Minor changes in EOP can be partially corrected analytically using of the projective transformation (2-25) through fixed control points, while it is necessary to respect geometric predispositions of this transformation, as all points should lie at least approximately in the same plane.

$$X = \frac{a_1 x' + a_2 y' + a_3}{c_1 x' + c_2 y' + 1}, Y = \frac{b_1 x' + b_2 y' + b_3}{c_1 x' + c_2 y' + 1} \qquad (2-1)$$

where *X*, *Y* are the reference coordinates-image coordinates measured in zero state, *x´*, *y´* are image coordinates of a given epoch, and *a1 – c2* are transformation coefficients [3]. Projective transformation was chosen, because this type of transformation includes the attributes of both similarity and affine transformation, while it also enables the plane of the image to tilt [18] which partially solves the orientation problem presented in section 2.4 and the self-heating problem presented is section 2.1.

2.5.3 Testing the stability of cameras

A series of experiments was conducted, first measuring image coordinates using a physically stabilized camera without analytical stabilization. Then, the captured images were processed again, this time incorporating analytical stabilization. The images from the experiment detailed in section 2.1 were reused, and the experiment was replicated with three additional cameras. These cameras were used to measure the 25-pixel diameter targets.

The battery in the Leaf Aptus-II 12 lasted less than 40 minutes and had to be changed twice, and this caused a slight shift in camera position, therefore the results had to be corrected by continuing the graph where it left off before the swap. The digital back of the camera was also equipped with a small fan, which cooled the sensor, however this cooling effect seemed inconsistent based on significant variations. The deviations from zero are high compared to the other camera models, and the variations in image coordinates far exceed the required accuracy of 0.1 pixels, therefore the Leaf Aptus-II 12 isn't suitable for deformation measurements where high accuracy is required, therefore was eliminated on this basis from further testing.

It is also notable that among the three other cameras, the deviations induced by the self-heating effect are the highest in the Sony A7RIII, however it seems like it levels out at the two-hour mark. The statistical analysis for the changes in image coordinates for different cameras is shown in table 2.1.

Tab. 2.1 Changes in image coordinates for different cameras

Statistics for t=120 min until t=180 min (pix)										
Camera	Mean value		St. deviation		RMS		Min		Max	
	X	Y	X	Y	X	Y	X	Y	X	Y
D850	0.001	0.004	0.005	0.004	0.005	0.006	-0.007	-0.007	0.012	0.013
D7500	0.007	0.013	0.015	0.013	0.017	0.019	-0.025	-0.013	0.042	0.056
A7RIII	-0.129	-0.030	0.051	0.038	0.139	0.048	-0.250	-0.108	0.000	0.084

According to the standard deviation, and maximum/minimum values in table 2.1, the Sony A7RIII camera isn't suitable for high-accuracy deformation measurements without corrections using transformation. This camera is equipped with 5-axis optical in-body image stabilization which compensates for vertical/horizontal shift and yaw/pitch/roll [19]. Even though this feature was disabled during the experiment, it might have been partly responsible for the significant changes in measured image coordinates, however this statement requires further testing.

The Nikon D7500 camera produced promising results, however it lacks the “silent shooting” function, which might have caused the more pronounced variations in image coordinates. Overall, this camera could be used as a cheaper substitute for the D850 when measuring deformations.
The images acquired during the experiment were processed again. 8 targets and 4 control points were measured this time. The results obtained are the results for the first 120 minutes of the experiment, as this is the stage where the self-heating phenomenon is the most prominent.
The RMS of residuals remained consistent across cameras and targets; however, the calculations have proven the reliability of the Nikon D850 camera again. Based on the statistical analysis, the measured coordinates affected by self-heating during the first 120 minutes, were sufficiently corrected using projective transformation.

2.5.4 Flash vs silent shooting

Using flash in photogrammetry, especially with reflective targets, offers distinct advantages. It enhances contrast and diminishes background brightness, thus minimizing the likelihood of edge detectors encountering false edges. However, utilizing a flash necessitates the use of a mechanical shutter. In this mode, the mirror flips up, and the shutter opens to expose the sensor to the light coming through the lens before closing again.
Silent shooting, an alternate mode, holds the potential to reduce vibrations during image capture. In this setting, the mirror remains locked in an upward position and the shutter stays open. The camera uses the image sensor itself to capture the image, eliminating physical shutter movement. Nonetheless, it's crucial to note that most cameras, due to synchronization challenges, cannot support simultaneous usage of an electronic shutter and flash.
In the context of this study, an experiment was conducted using a remotely operated Nikon D850 camera equipped with a mounted flash. The experimental procedure involved capturing a series of images: first, 10 without flash in silent-shooting mode, followed by 10 with flash, and then sequences of 5, 3, 2, 2, 1, and 1 image. Eight points and four control points were measured in this experiment. Despite the evident influence of flash on coordinate measurement, projective transformation used for analytical correction minimizes this effect.

2.6 Determining target scale

The size of the pixel projected on the object determines the scale of the measured displacements and enables the direct calculation of the displacement size from the image coordinates. Four approaches were tested for determining target scale:

1. Determining from scale bar.
2. Interpolation from scale bar to other points.
3. Normal distances of targets from the image plane.

The difference between the three methods is negligible.

2.6.1 Impact of incorrectly determining targets scale

Determining scale using normal distances is quite a straightforward approach, however, the other two methods might induce some problems when calculating scale if the scale bars are tilted or the two pairs of control points are fixed on a slanted object. If the scale bar tilts towards or away from the camera, it will appear shorter in the image, if the base of the bar remains at the same distance from the camera. A tilt of 10° would change the projected length to 98.5 pixels and the GSD to 10.15 mm.

2.7 Correcting images for lens distortion

Radial symmetric distortion will affect the results if it affects the image coordinates by more than 0.05 pixels between epochs. The size of the error from lens distortion depends on the course of the radial distortion, the position of the observed point in the image, and the amount of displacement of the point in the image between individual phases. Therefore, before the experiment, it is necessary to calculate the theoretical values of this error with respect to the observed object, and if they exceed the accuracy of the measurement of image coordinates, it is necessary to calibrate the camera and use redrawn images or introduce correction analytically [3]. As the author’s algorithm for deformation measurements in real time is coded in MATLAB, the built-in **Camera Calibrator** app was used.

3 Online measurements of deformations and displacements using time base photogrammetry

This chapter presents the algorithm that the author has developed. The purpose of this algorithm is to measure deformations and displacements using online time base photogrammetry. Although the method was primarily designed for bridge load tests, it's versatile enough to be applied to various objects' load testing without the necessity of changing the code. The algorithm is comprised of five main components:

1. Camera calibration
2. Target stabilization
3. Camera configuration
4. Measurements
5. Results computation

The following subsections will explain each step in detail. They provide comprehensive instructions to guide future users in effectively and accurately utilizing this software.

3.1 Camera calibration

Camera calibration follows the procedure defined in Section 2.7, employing the MATLAB Camera Calibrator app. Users are only required to specify the sensor size (in millimeters) and the path to the calibration protocol, specifically the .mat file generated during chessboard calibration. Lens distortion can be significant, especially when using medium to wide-angle lenses [20]. Therefore, it is generally recommended to correct images for lens distortion. Nonetheless, images taken with high-quality lenses may not necessitate such correction, as these lenses typically exhibit minimal distortion. Any residual distortion can further be mitigated during the application of a projective transformation to the coordinates measured in the image.

3.2 Target stabilization

The placement of targets and control points should be determined in consultation with the structural engineer responsible for the load test in question. As discussed in section 2.6, the algorithm supports three methods for scale calculation. If the object under test is thin, making it problematic to attach scale bars, it is recommended to define scale using two pairs of control points or based on the measured real-world coordinates of the targets and control points. The provided adhesive stickers, which are also used for the scale bars, can adhere to practically any dry surface. To choose the appropriate scaling method, the following factors should be taken into consideration:

1. When all targets and control points lie in the same plane, it is sufficient to interpolate scale from the known distance between control points. The distance between pairs of control points does not necessarily have to be equal.
2. If the points are not all in the same plane or if the control points cannot be vertically aligned, it is more appropriate to use the scale bar method.
3. When both control points and targets are at various distances, it is necessary to use a total station to measure the XYZ coordinates of the targets and control points.

3.3 Setting up the camera

3.3.1 Stabilization and preparation

As elaborated in section 2.5, the camera should be physically stabilized. It should be levelled using the mount's leveling screws, based on the virtual horizon, ensuring that the optical axis is directed towards the object's center. Lens selection is a task that requires careful consideration, considering both the dimensions of the object under examination and the distance to the object. This choice should coincide with the camera selection intended for the measurements, as described in Section 2.2.

Next to the camera, the notebook equipped with all necessary software should be situated. A foldable music stand for sheets could be an ideal choice for this purpose, although numerous options exist, and the placement of the notebook depends on the specific circumstances. In the case of the Nikon D850, the camera is tethered to the notebook using a USB Micro Type B cable [21]. Unfortunately, this cable does not facilitate camera charging, hence during extended load tests, battery replacement might be needed. More recent cameras, for example, the Sony A7RIII, support control, data transfer, and charging via USB-C [22]. If the load test is conducted in the field, a power bank is necessary. The VIKING X-1000 power station was employed for this thesis and it lasted approximately 10 hours while charging an HP OMEN notebook equipped with an i9 Intel processor, and subsequently, a Sony A7RIII camera via the notebook (explained in detail in section 3.5). The solar panel system was not tested but could potentially be utilized outdoors to extend the battery life further.

3.3.2 Capture settings and threshold

The camera settings, including aperture, ISO, and shutter speed, need to be carefully configured to ensure optimal image quality for measurement. The aperture should be carefully set to maintain sharp focus throughout the image. This setting depends on the camera's orientation relative to the object being measured. Generally, an f-stop of 8 is suitable, but this choice should be adjusted based on the specific situation and the desired shutter speed. Low ISO settings are preferred for two reasons: firstly, they reduce image noise – although tests have proven that the Edge-ellipse operator is robust against noise; secondly, low ISO settings lead to shorter exposure times. With flash photography, the exposure time typically cannot be shorter than 1/250 seconds. A higher ISO would result in brighter, potentially overexposed images when using a flash, leading to inaccuracies in edge projection, and therefore edge detection.

When using flash, it's important to adjust the aperture, ISO, and shutter speed such that the reflective targets are clearly visible and dominant in the image, without causing overexposure.

The file format should be chosen in accordance with section 2.3. Proper camera settings and flash use will yield consistently bright targets and control points against a darker background. This facilitates the use of the Edge-ellipse operator, as the targets and control points will be the brightest objects in the image, exhibiting the largest intensity changes at edges.

3.3.3 Camera control and data transfer

An array of camera controlling software options exists, however, verifying compatibility with the specific camera and image format is essential as certain programs may encounter difficulties when transferring raw or tiff files. Numerous camera brands offer their own camera controlling software, for instance, Sony's Imaging Edge Desktop [56], which is free to use. Additionally, other open-source software options such as digiCamControl [23] are available, which facilitate camera controlling and image transfer. In general, the specific software used is of little consequence as long as it allows basic camera settings to be controlled via the computer and the captured images can be transferred to a selected folder on the PC's memory. The utilization of proper software results in the image appearing in the specified folder within mere seconds.

3.4 Carrying out measurements

Following the necessary preparatory steps, the first image can be captured and will be automatically transferred to the preselected folder on the PC. This section outlines the automated workflow, which does, however, require certain user inputs during setup.

Before running the program, either the dimensions of the scale bars must be known, or the coordinates of the targets and control points should be measured using a total station. The distances between the targets on the supplied scale bars are 800 mm. The distances between two pairs of control points should be measured, for example, using a measuring tape.

At this point all the necessary preparations are complete and the user may capture the first image of the object using the interface of the software of choice.

3.4.1 Running the code – initialization and user input

For the sake of clarity, the code will be explained using images acquired during a load test performed in Kunov, Slovakia. Let's consider that the image of the zero state was already captured.

At this stage, the MATLAB code can be executed. Upon pressing the 'run' button in MATLAB, a prompt appears for the user to select the zero-state image. Utilizing the familiar interface of Windows Explorer, the user can easily select this image. The code then decomposes the filename, returning each component.

The this point the image that captures the object with no load applied is read into MATLAB. In the next step, a pop-up window queries the user about the desired method for defining scale. In the following step, the user is given the option to load target and Control Point (CP) selections from an .xlsx file, or to manually select the targets on the image. If the user opts to manually select the targets on the image, the calibrated image is displayed, and the user draws rectangles around the desired targets (fig 3.3) before hitting the 'escape' key. Rectangles are drawn by clicking and holding the left mouse button (LMB) at a chosen point, dragging the rectangle around the target, and then releasing the LMB. It is critical to draw the rectangles such that the targets remain within bounds even after deformations occur. When deformations happen, care should be taken to ensure no false edges (edges not part of the target edge) fall within the bounds.

The calibrated image shows again, and the same process is repeated for the control points. The `imgzoompan` function by Dany Cabrera [24] is used to facilitate a more intuitive manipulation of the image, such as zooming using the mouse wheel and panning by holding the right mouse button (RMB). If no CPs are selected, the scale definition using CPs won't work, and no analytical stabilization will occur later in the program. At this point, all data about the drawn rectangles are stored in an .xlsx file named lastCoordinates.xlsx in the directory.

If the user decides to load coordinates from an .xlsx file, the Windows Explorer interface opens, providing the option to select the file of interest. This could be a previously saved 'lastCoordinates.xlsx' or a manually edited file with an identical structure and optionally, a different filename. The user will also encounter a pop-up window prompting them to specify the distance between targets or between CPs. Should the user decide to define scale using perpendicular distances, they are immediately asked to select the .xlsx file containing the coordinates.

The default value stands at 800 millimeters, given that this figure corresponds to the size of the supplementary scale bars. For the processing to function correctly, it is imperative that the scale bar points are selected sequentially: the first point (T1) of the first scale bar is selected first, followed by the second point (T2) of the same scale bar, subsequently the first point (T3) of the second scale bar, and finally the second point (T4) of the second scale bar, and so on. Likewise, one should first select the two CPs positioned above each other, followed by the second pair of CPs.

3.4.2 Running the code – automatized processing

Automated processing begins at this stage. For each captured image, the algorithm proceeds through several steps:

1. Measurements of targets are undertaken as described in section 2.1.
2. Analytical stabilization is carried out as outlined in section 2.5.
3. The algorithm calculates the deformation compared to the zero-state coordinates by subtracting the image coordinates of targets measured in the zero-state image from those measured in the currently processed image.
4. The scale for each target is calculated as detailed in section 2.6.
5. The vertical deformations are converted into real-world deformations, employing the scale factor for each target.

These deformations are subsequently displayed in a live plot and a table that is refreshed after each iteration, i.e., after each instance of image capture. Once the live plot and the table pop up, the user may arrange these windows on the screen. A suggestion for this arrangement is the following: the live plot with the legend predominates the screen, the scrollable table of vertical deformations is positioned adjacent to the live plot, and the camera controlling software, in this instance digiCamControl, is placed next to it.

In the current version of the software, when the number of calculated epochs exceeds 100 on the X-axis, the live plot defaults to display only the most recent 100 epochs. To adjust this limit according to user preference or display size, the value of `xPlotLimit` – currently set at `xPlotLimit = 100` – should be modified.

Furthermore, three .xlsx files are generated for each iteration:

- ‘All Subpixel Coordinates.xlsx’ contains the raw measured image coordinates of points.
- ‘Transformed Ellipse Center Coordinates.xlsx’ includes the transformed image coordinates.
- ‘Vertical Deformations mm.xlsx’ holds the vertical deformations in millimeters.

These files serve two main purposes. Initially, they function as a safety measure, ensuring that in case of a field issue such as the notebook's battery depletion, the coordinates are preserved and can be utilized once the issue is rectified. Secondly, they facilitate further analysis in Excel.

The MATLAB code then increments the image number by one, compiles the filename of the new image based on the prefix, suffix, and new image number, and checks whether this image already exists in the directory. If it does not, the program waits and checks again.

In some cases, the filename may already appear in the directory while the file is still being transferred. If the software attempts to read this partially transferred or empty file, it would crash. To avoid this, once the filename appears in the directory, the program waits for a second to ensure the file is fully transferred. One second has been found to be a sufficient buffer to avoid a crash.

Once the new image is loaded into MATLAB, the process is repeated until the code is stopped. The only user interaction required at this stage is clicking the ‘capture’ button in the camera control software. The rest is automated. The capturing process can also be automated by selecting the ‘interval shooting’ mode.

3.5 Laboratory tests of the algorithm

The accuracy and reliability of the algorithm have already been demonstrated through the tests performed in chapter 2. Some of these tests, conducted using an earlier version of the algorithm, have been recalculated with the current version for consistency. To further illustrate the functionality of the code, two additional laboratory tests have been conducted to simulate practical field situations. The first test employed a SONY A7RIII camera with a 35 mm lens. These tests were conducted within a laboratory environment. The camera was positioned on a camera tripod (not a heavy surveying tripod) and connected to an HP OMEN laptop using a USB-C cable. The laptop was powered by a VIKING X-1000 power station. Given the capabilities of a USB-C cable, the camera was charged concurrently. Every five minutes, from 12:50 until 15:40, an image was captured (35 images in total), then the setup was slightly adjusted, and a new set of measurements was carried out from 17:00 until 22:30. The measurements stopped because first the power station and then the notebook ran out of batteries. Again, the hypothesis was that the points are stationary, and the measured deformations should be zero. The test was carried out using analytical stabilization on four CPs with no calibration.

The results of this experiment demonstrate that high accuracy can be maintained even after prolonged measurement campaigns. The results align with those previously obtained, as presented in table 2.1. As in earlier experiments, the RMS of the X values is notably higher than that of the Y values for the Sony A7RIII. However, this discrepancy does not impact the measurement of vertical deformations. The RMS values in axis Y never exceeded 0.05 pixels, which is way beyond the desirable accuracy of 0.1 pixel. Only in two instances did the minimum/maximum values for the vertical displacements exceed 0.1 pixel, once on target T7 and once on T8. The experiment also demonstrated that, when powered by the mentioned power station, this configuration can operate for up to 9 hours and 40 minutes. It should be noted that the camera's sensor wasn't perfectly parallel to the wall bearing the targets but pointed at the wall at an approximately 15° angle. While the increased RMS in the experiment outlined in Section 2.5.3 could potentially have resulted from a self-heating phenomenon, no analytical stabilization was applied in that case. The potential influence of the smaller secondary axis of the projected ellipse on the uncertainty in measuring the X coordinates merits further investigation.

To explore this further, a subsequent experiment was conducted using the D850 camera equipped with a 35mm lens. In this instance, both calibration and analytical stabilization were carried out using the CPs. One image was captured every minute over a span of 110 minutes. A total of 14 targets were measured.

The highest RMS value for vertical deformations was observed on target T9, with the RMS values for the other targets being significantly lower. In all instances, the RMS for the deformations in the X axis was larger than in the Y axis, suggesting that the smaller secondary axis of the ellipse might result in less precise measurements in the X axis. It's worth noting that when the camera is set up with a horizontal optical axis, the primary axis of the ellipse will always be vertical, hence the vertical deformations will be measured with higher accuracy. The statistical analysis concluded that measurements exhibit similar accuracy in both X and Y axes for the same camera-lens configuration, hence, the smaller secondary axis of the ellipse is accountable for the diminished accuracy in the X axis. In this instance, the worst RMS value was 0.03 pixels.

3.6 Field tests

A series of field tests were carried out using the Nikon D850 and the Sony A7RIII cameras. Two load tests of two newly built bridges were carried out, one in Kunov and one in Holíč, Slovakia. The load test in Kunov was also carried out using a lighter sport utility vehicle (SUV) instead of a loaded truck.

3.6.1 Load test in Kunov

The first load test took place on a bridge in Kunov. The Nikon D850 camera was positioned on one side of the bridge, while the Sony camera was placed on the other side. In both scenarios, four Control Points (CPs) were utilized. The Nikon D850 captured six targets, T1 through T6, and The Sony A7RIII captured two targets, T7 and T8. Precision leveling near the targets was conducted using the Trimble DiNi leveling instrument [25], which provides height measurement resolution of 0.01 mm. The scale was determined based on the known length of the scale bars, which was 830 mm. Given the camera setup and an approximate distance of 30 meters, the anticipated accuracy of the photogrammetric measurement should have been around 0.20 mm. However, the highest RMS value achieved using the D850 camera was 0.44 mm, which is notably higher. However, there are two important factors to consider that could contribute to this discrepancy:

1. The timing of the measurements: The photogrammetric and leveling measurements were not conducted simultaneously. This time differential could introduce discrepancies due to dynamic factors affecting the bridge. For instance, changes in environmental conditions such as temperature fluctuations, wind action, or even vibrations caused by pedestrian activity on the bridge could induce slight shifts in the bridge's position between the two measurements.
2. Spatial alignment of measurement points: The specific points used for photogrammetry and leveling were not identical. Any distance between these two points could lead to differences in the deformation measurements, particularly if the deformation across the bridge is non-uniform.

Both of these factors could potentially lead to variations in the measured deformations between the two methods, even if both methods are intrinsically accurate. It's also worth noting that while the 0.44 mm RMS value is higher than the anticipated 0.20 mm, it still represents a high degree of precision for many practical applications.

3.6.2 Load test in Holíč

A load test was undertaken in Holíč on a newly constructed cyclist bridge, which was completed in 2023. This time, a 0.5 m long levelling rod was directly attached to the scale bar, leading to the expectation that any displacement on the scale bar would correspond to the same displacement on the levelling staff. Unfortunately, severe weather conditions posed a challenge; measurements were conducted during a storm. To prevent potential damage to electronics caused by rain, the online measurements had to be suspended midway through the load test.

3.6.3 Second load test on the bridge in Kunov

A second load test was executed on a military bridge in Kunov, utilizing a Nikon D850 camera equipped with a 35 mm lens. The camera was positioned at a distance of 27.6 meters, resulting in a GSD of 3.4 mm. The camera was physically stabilized using a heavy surveying tripod. For this test, a smaller 2-ton car was used to load the bridge. 0.5-meter long leveling staffs were attached to each scale bar. Reflective targets were also employed this time.

The procedure followed the steps of performing the zero-state measurement, followed by three cycles of loading and unloading the bridge. During each leveling measurement taken for each leveling staff, an image was simultaneously captured. This procedure resulted in three images for each state, with the exception of the first loaded state, enabling a better correspondence between the photogrammetric and leveling measurements. The differences in vertical deformations measured using the two methods and the statistical analysis are shown in table 3.1.

Tab. 3.1 Differences in vertical deformations measured using the two methods and the statistical analysis

Nikon D850 – Trimble DiNi							
	ID	T1	T2	T3	T4	T5	T6
Differences between measured deformations (mm)		0.00	0.00	0.00	0.00	0.00	0.00
	Load	0.21	0.13	0.22	0.28	-0.03	0.09
	Load	0.04	0.04	0.09	0.11	-0.05	-0.14
		0.08	0.30	0.06	0.07	-0.14	-0.09
		0.36	-0.01	-0.02	0.54	-0.05	0.00
		-0.17	0.08	0.13	0.11	-0.07	-0.03
	Load	0.17	0.18	0.09	0.21	0.24	0.13
	Load	0.05	0.09	0.06	0.06	0.05	0.06
	Load	0.01	0.00	0.07	0.01	0.09	0.06
		0.11	0.30	-0.15	0.29	-0.02	0.36
		0.38	0.43	0.03	0.08	0.06	0.16
		0.09	0.24	0.10	0.13	0.07	0.19
	Load	-0.39	-0.13	-0.25	0.00	-0.20	-0.61
	Load	-0.09	0.11	0.02	0.09	-0.09	0.03
	Load	0.05	0.04	-0.11	0.07	-0.17	-0.31
		-0.07	-0.08	0.09	0.11	0.10	-0.25
Stat. analysis	Avg.	0.05	0.11	0.03	0.13	-0.01	-0.02
	Min.	-0.39	-0.13	-0.25	0.00	-0.20	-0.61
	Max.	0.38	0.43	0.22	0.54	0.24	0.36
	St.dev.	0.18	0.14	0.11	0.13	0.11	0.22
	RMS	0.19	0.18	0.12	0.19	0.11	0.22

Given a distance of 27.6 m and using a 35 mm lens on a Nikon D850 camera, the expected accuracy should be around 0.17 mm. The most significant differences between levelling and photogrammetry were 0.54 mm and -0.61 mm. Unfortunately, the RMS reached up to 0.22 mm on T6; however, when converted to pixels, this value is still better than 0.1 pixels, which was the primary goal. Yet, when considering all differences between measured deformations, the global RMS is 0.17 mm, which equates to an accuracy of about 0.05 pixels.

It's important to note that the deformations measured at the two ends of the scale bars do not match, although they were expected to. This discrepancy might be due to the tilting of the scale bars as the object deformed. It is also important to keep in mind that, as before, it's physically impossible to capture the images at the exact same moment as the leveling is performed. Furthermore, smaller, and less rigid bridges are susceptible to deformation.

4 Results and discussion

The primary objective of this dissertation revolved around the design and implementation of a system for online processing of photogrammetric measurements of deformations and displacements. The photogrammetric method employed was time based photogrammetry, an approach that encompasses capturing images of objects from a singular camera with constant IOP and EOP. The subsequent stage involves comparing the image coordinates measured in the images with those derived from the zero-state image. In order to carry out precise and accurate measurements, the following prerequisites must be fulfilled:

1. Utilization of a target measuring operator boasting an accuracy exceeding 0.1 pixel.
2. A high degree of spatial and geometric resolution.
3. Superior image quality.
4. Ensuring that the image plane aligns parallel to the deformation plane.
5. Constant EOP and IOP, implying a stable camera.
6. Accurate computation of the scaling factor.
7. Images that have been corrected for lens distortion.

To meet these requirements, an image coordinate measuring operator was developed. This operator utilizes the subpixel edge detection method based on the partial area effect, developed by Trujillo-Pino, and a least square ellipse fitting function developed by Richard Brown. This Edge-ellipse operator is outlined in detail in section 2.1, where its performance was also validated.

In an idealized environment under laboratory conditions, an array of experiments was conducted using various cameras and target sizes. The measurements were carried out repeatedly over several hours, capturing an image every minute. Both the cameras and the target board were bolted to a steel plate. By employing the Nikon D850 camera in conjunction with the Edge-ellipse operator, an accuracy of up to 0.005 pixels was achieved. When assessing targets of varying diameters, the most accurate were the 50-pixel diameter targets, closely followed by the 25-pixel diameter targets.

The Edge-ellipse operator demonstrated an accuracy level comparable to both the LSM method and DIC. However, the LSM method failed to measure the smallest targets, those with a diameter of 5 pixels. In a separate experiment, a limitation of the DIC method was exposed: when numerous similar targets are present in the image, the correlation algorithm may mistakenly associate certain targets. Therefore, the newly developed Edge-ellipse image coordinate measuring operator measures up to current standard operators.

The spatial and geometric resolution directly influences the GSD value, which subsequently impacts the accuracy of measurements in real-world coordinates. The accuracy of the method, based on the distance between the object and the lens, is demonstrated with the Nikon D850 camera, which yielded the best results.

The assessment of image quality within various settings revealed that even though the Edge-ellipse operator exhibits resilience against noise, it is advisable to maintain the ISO value at 100. This ensures that when using flash, the images do not become overexposed, given that the shortest exposition time when utilizing flash is 1/250. A high f-stop, indicative of a small aperture, did not trigger noticeable lens diffraction.

During measurements, the importance of ensuring a horizontal optical axis becomes paramount, thereby guaranteeing a vertical image plane. This ensures that alterations in Y image coordinates can be accurately converted to true vertical deformations.

As the algorithm was constructed within MATLAB, it was fitting to employ the software's built-in camera calibrator app, partly due to the proven effectiveness of the chessboard calibration method in determining camera IOP. For camera stability, physical stabilization must be combined with analytical stabilization. In terms of physical stabilization, a surveying tripod with an adapter was found to be adequate. Projective transformation, using four control points, emerged as a reliable method for rectifying even small changes in image coordinates, such as self-heating effects that appear as sensor tilting. Based on the calibration protocol, images can also be rectified for lens distortion, although this may not be necessary in all instances.

The author's algorithm includes three methods for determining scale:

1. Using target scale bars
2. Using known distances between vertically aligned control point pairs
3. Using the measured XYZ coordinates of points

The first two methods rely on measuring the pixel distance between point pairs when the real-world distance is known, enabling the calculation of GSD. The third method utilizes image resection based on the measured image coordinates of points and their corresponding real-world coordinates.

The aforementioned solutions were integrated into a MATLAB code, which also facilitated the interpretation of deformations via a live plot that updated after each iteration. A side table was incorporated to enable easier user comprehension of the results.

Several reliable and proven camera control software options were examined. However, the digiCamControl software, due to its open-source nature and comprehensive functionality, is recommended. The software-hardware configuration underwent rigorous experimental validation in both laboratory and field settings. Despite the fact that the RMS value occasionally exceeded 0.1 pixel when compared to precise leveling with an accuracy of 0.01 mm, the attained results of the Sony A7RIII camera still maintained an accuracy of under a millimeter. However, these results were subject to distortion due to three factors:

1. Timing of the measurements.
2. Spatial alignment of measurement points.
3. Adverse weather conditions.

When repeating the measurements using the Nikon D850 camera with a 35 mm lens the accuracy has improved. Here, the global RMS of all differences between the photogrammetric measurements and leveling was 0.17 mm, which for a distance of 27.6 m corresponds to 0.05 pixels. Unfortunately, when comparing photogrammetry with leveling, it is not feasible to conduct the measurements with the exact same timing or to measure precisely the same points, as both methods are founded on differing principles, resulting in at least some variance in targets – leveling rod versus circular reflective target. While load tests are not typically conducted in adverse weather, changing lighting conditions are a natural occurrence during measurements, however, it was established that such changes do not significantly affect the Edge-ellipse operator.

4.1 Limitations of the solution and suggestions for further research

Certain observations have indicated that when the horizontal optical axis is angled towards circular targets, the accuracy of the X coordinates may be compromised when compared to the Y axis. This phenomenon could be due to the secondary axis of the fitted ellipse being relatively smaller than the primary axis. Although this was theoretically proven in section 3.5, it necessitates further testing.

Without using reflective targets and when deformations surpass the buffer zone of the plastic plate on which the reflective targets are affixed, false edges may be detected. This issue can be mitigated by using a camera flash and setting an appropriate threshold value. These actions will ensure that reflective targets are brightly illuminated (but not overexposed) when the correct shutter speed is set, resulting in sharp edges. Therefore, the only edges detected will be those of the targets.

One limitation of the current code version is that when calculating the scale using two CP pairs, no additional CPs can be used for analytical stabilization. When calculating scale using image resection, the XYZ coordinates of all targets and CPs should be known. More than four points might be necessary when the CPs are not distributed correctly, or maximum stability needs to be achieved. This is a straightforward programming issue that can be resolved quite easily if needed, with some CPs used to define scale and some additional CPs aiding in analytical stabilization. However, when scale definition is based on target scale bars, any number of CPs can be used.

The speed of the software is heavily reliant on the hardware. Typically, it takes 2-5 seconds to measure a target, but this time can be reduced with notebooks equipped with superior cooling systems or higher performance capabilities. The speed of image transfer is contingent on the tethering software and the cable used, but it usually takes only a few seconds to transfer even large images from camera to computer. As wireless solutions evolve and become more reliable, a shift to wireless camera control and transfer could be possible without code alterations.

At present, the interpretation of results in the live plot and table primarily focuses on vertical deformations, whereas horizontal deformations can only be accessed from the generated Excel tables. This can be addressed with minor modifications to the code.

A possible enhancement of the algorithm would involve capturing images of dynamic deformations occurring rapidly. The ISO could be significantly increased, as it does not noticeably affect measurements up to a certain point. The aperture could be widened, and thus the shutter speed would substantially increase, resulting in sharp images of targets and CPs even during dynamic phenomenons. For instance, the Nikon D850 camera's top continuous shooting speed at full resolution is 7 frames per second; however, by reducing the resolution to 4K or full HD, it can capture images at framerates of 60 and 30 respectively.

To further augment analytical image stabilization, in addition to CPs, stabilization based on fixed regions in the image could be implemented. This would require cross-correlation, enhanced by interpolation (e.g., Gaussian peak interpolation). A portion of this is already incorporated into the MATLAB code, where the user can select the region in the background for projective transformation alongside the CPs. This selection can be found in the code under 'Get Natural Control Points'. The selection process is identical to the selection of targets and CPs; one simply needs to remove the "%} %{". This form of stabilization is already operational in the code, but its accuracy needs refinement, specifically fine-tuning of the interpolation function at the end of the code, known as 'fit2DGaussianToPeak'.

Another use of correlation is target detection. At present, users must exercise caution to avoid including false edges while drawing rectangles around targets and CPs. Cross-correlation could be employed for target detection when the deformations are substantially larger than anticipated during a load test. Initially, the targets need to be pinpointed with pixel-level accuracy using the built-in 'normxcorr2' function in MATLAB, followed by refining the target position using the Edge-ellipse operator. This correlation-based target detection is already encoded in MATLAB under the comment line '`%% If the deformations are large enable correlation and delete %{ %}`'. However, this component was not included in the final code because cross-correlation tends to

slow down the algorithm. It becomes unnecessary when the camera is adequately stabilized, both physically and analytically, and the deformations remain smaller than the buffer zone around the targets and CPs.
Finally, the existing code could be transcribed into Python or any other programming language as per the preference of the intended user base.

Conclusion

The primary objective of this dissertation thesis was to design and implement a system for online processing of photogrammetric measurements of deformations and displacements with minimal delay, conducted simultaneously with the ongoing image acquisition process. The specific objectives were the following:

1. Design of the optimal method of data transfer from the camera to the computer.

This task was completed by implementing several camera control software programs, most notably digiCamControl, which facilitated the control of the camera and automatic image transfer to a specified folder on the PC.

2. Selection of a suitable image operator and edge detector and their implementation, including subpixel measurement of mark centers.

For this purpose, the Edge-ellipse operator was developed, which makes use of an edge detection method that expects the edge to be curves, which is ideal for circular target measurements, and a least squares ellipse regression function that fits a regression ellipse over the edge coordinates. The accuracy of the Edge-ellipse operator reached up to 0.005 pixels, which far exceeded the previously specified required accuracy of 0.1 pixels.

3. Hardware and analytical camera stability solution.

Physical stabilization was achieved using a heavy-duty surveying tripod equipped with a camera adapter attached to a surveying mount. Analytical stabilization was conducted via projective transformation, which also corrected errors resulting from the camera's self-heating.

4. Graphical user interface design for data collection and processing.

The user interface was designed as popup windows for user inputs. The measured deformations are instantly plotted on a live plot and displayed in a live table. The algorithm also utilizes the interface of the camera controlling software.

5. Experimental verification of the system.

The system was validated in both laboratory and field settings with two cameras, the Nikon D850 and the Sony A7RIII. Tethered shooting using a cable proved to be more reliable than Wi-Fi, as no disconnections occurred when using the cable.

6. Analysis of the quality of measured data and the accuracy of displacements and deformations.

The Nikon D850 camera, equipped with a 35 mm lens, delivered high-accuracy measurements. Even after image undistortion and analytical stabilization, the worst RMS value of supposedly unchanged coordinates was 0.03 pixels in laboratory settings. The configuration was also field-verified, which resulted in a 0.05-pixel RMS when compared to levelling measurements performed using the Trimble DiNi levelling instrument. This corresponds to a 0.17 mm discrepancy measured from a 27.6-meter distance. However, various factors could have contributed to the discrepancy, such as timing differences between the two methods and different spatial alignment of measured points.
In conclusion, all objectives of the dissertation thesis were not only met but surpassed. A combination of software, hardware, and camera configuration resulted in a system enabling efficient camera control, almost instantaneous data transfer, and target measurements with up to 0.005-pixel accuracy taking only 1-5 seconds per target. Given the ongoing advancements in camera and computer technologies, improvements in processing speed and accuracy are anticipated. Additionally, the potential for enhanced wireless data transfer could be realized without necessitating any modifications to the existing code. The algorithm that has been developed is characterized by its accuracy, reliability, and significant potential for future enhancements.

Literature

[1] ABOLHASANNEJAD, Vahid, et al. Experimental Evaluation of Deformation of Transport Infrastructures using Image-based Methods.

[2] ABOLHASANNEJAD, Vahid; HUANG, Xiaoming; NAMAZI, Nader. Developing an optical image-based method for bridge deformation measurement considering camera motion. *Sensors*, 2018, 18.9: 2754.

[3] FRAŠTIA, M. *Vybrané aplikácie fotogrametrie v oblasti merania posunov.* Habilitačná práca. 2017.
[4] HUANG, Jinke, et al. Measurement method and recent progress of vision-based deflection measurement of bridges: a technical review. Optical Engineering, 2022, 61.7: 070901-070901.
[5] KOPÁČIK, A.: *Meranie posunov a pretvorení stavebných objektov.* In: Vybrané geodetické a kartografické činnosti vo výstavbe, Komora geodetov a kartografov Bratislava, ISBN 978-80-89623-02-0
[6] STN 73 0405 Measurement of deformation of building constructions. 2022.
constructed facilities, 2004, 18.4: 213-219.
[7] LUHMANN, Thomas, et al. Close range photogrammetry. *Whittles, Caithness*, 2006.
[8] DZ Turner, Digital Image Correlation Engine (DICe) Reference Manual, Sandia Report, SAND2015-10606 O, 2015
[9] TRUJILLO-PINO, Agustín, et al. Accurate subpixel edge location based on partial area effect. Image and Vision Computing, 2013, 31.1: 72-90.
[10] Agustin Trujillo-Pino (2021). Accurate subpixel edge location (https://www.mathworks.com/matlabcentral/fileexchange/48908-accurate-subpixel-edge-location), MATLAB Central File Exchange. Retrieved May 11, 2021.
[11] Richard Brown. fitellipse.m, MATLAB Central File Exchange. [000 Online] 2021 [000 Accessed April 13, 2021] Available at: https://www.mathworks.com/matlabcentral/fileexchange/15125-fitellipse-m.
[12] MA, Shaopeng; PANG, Jiazhi; MA, Qinwei. The systematic error in digital image correlation induced by self-heating of a digital camera. Measurement Science and Technology, 2012, 23.2: 025403.
[13] MA, Qinwei; MA, Shaopeng. Experimental investigation of the systematic error on photomechanic methods induced by camera self-heating. Optics express, 2013, 21.6: 7686-7698.
[14] YU, Liping; LUBINEAU, Gilles. Modeling of systematic errors in stereo-digital image correlation due to camera self-heating. Scientific reports, 2019, 9.1: 6567.
[15] FLIR Systems. "FLIR T620 | FLIR Systems." Available at: https://www.flir.com/support/products/t620/#Overview [Accessed: June 30, 2023]
[16] OBILOR, Esezi Isaac; AMADI, Eric Chikweru. Test for significance of Pearson's correlation coefficient. International Journal of Innovative Mathematics, Statistics & Energy Policies, 2018, 6.1: 11-23.
[17] PhotoModeler. [online] Available at: https://www.photomodeler.com/ [Accessed: June 30, 2023].
[18] MATLAB & Simulink. "Matrix Representation of Geometric Transformations." Available at: https://www.mathworks.com/help/images/matrix-representation-of-geometric-transformations.html [Accessed: June 30, 2023].
[19] Sony UK. "Sony ILCE-7RM3 | Full-Frame Mirrorless Camera." Available at: https://www.sony.co.uk/electronics/interchangeable-lens-cameras/ilce-7rm3 [Accessed: June 30, 2023].
[20] STEIN, Gideon P. Lens distortion calibration using point correspondences. In: Proceedings of IEEE Computer Society Conference on Computer Vision and Pattern Recognition. IEEE, 1997. p. 602-608.
[21] CARMINATI, Marco; LUZZATTO-FEGIZ, Paolo. Conduino: affordable and high-resolution multichannel water conductivity sensor using micro USB connectors. Sensors and Actuators B: Chemical, 2017, 251: 1034-1041.
[22] LI, Alan. Usb type-c for machine vision. Quality, 2018, 16VS-17VS.
[23] digiCamControl. [online] Available at: https://digicamcontrol.com/ [Accessed: June 30, 2023].
[24] Dany Cabrera (2023). Image Mouse Zoom and Pan (https://github.com/danyalejandro/imgzoompan), GitHub. Retrieved May 18, 2023.
[25] Trimble. "Datasheet - DiNi Digital Level - English (US)." Available at: https://geospatial.trimble.com/sites/geospatial.trimble.com/files/2020-11/Datasheet%20-%20DiNi%20Digital%20Level%20-%20English%20(US)%20-%20Screen.pdf [Accessed: June 30, 2023].